Electronic Supplementary Material (ESI) for RSC Advances

Supplementary Information for

Continuous gas-phase synthesis of metal oxide-graphene hybrid nanoflakes for the enhancement of lithium storage

Jeong Hoon Byeon and Young-Woo Kim

EXPERIMENTAL DETAILS

Fabrication process: Aerosol graphite nanoparticles were produced *via* spark discharge and carried by nitrogen gas (99.9999% purity, 3 L min^{-1}, Tylan, US) to an impinging device, as shown in **Scheme 1**. The impinging device, which contained a simplified Hummer's solution and an ultrasound probe (VCX 750, Sonics & Materials, US), was used to collect the graphite particles into the solution and react subsequently with the solution to form GO. The graphite particles (which acted as precursors) experienced ultrasound (250 W cm^{-2} in intensity) when they reached the gas (the graphite particle laden flow)-liquid (the simplified Hummer solution in the impinging device) interface. The reacted solution containing GO was injected into the reservoir of a collison atomizer using a peristaltic pump (323Du/MC4, Watson-Marlow Bredel Pump, US). The GO solution was atomized as droplets and then passed through a denuder containing activated carbon pellets and silica gels to drive solvent from the droplets. The GO particles were immersed in the other ultrasound-impinging device to be photoreduced as rGO. Another spark discharge was used to generate aerosol SnO_x nanoparticles, and the particle laden air flow (3 L min^{-1}, Tylan, US) was employed as the operating gas for atomizing the rGO solution supplied by the other pump. The SnO_x particles passed over the atomizer orifice, where they mixed with atomized rGO droplets to form hybrid droplets. The droplets then passed through a heated tubular reactor (GTF 12/25/364, Lenton Furnaces, UK) operating at a 90^{o}C wall temperature to drive water from the droplets. The resulting aerosol SnO_x-rGO hybrid particles were then collected to be employed as an active material of a LIB.

Spark discharge: To create aerosol graphite or SnO_x (MoO_x or NbO_x) particles, a spark was generated between two rods (graphite-graphite or metal-metal) inside a chamber in a pure nitrogen (or air for metal-metal) environment at standard temperature and pressure. The specifications of the discharge configuration were as follows: electrode (Nilaco, Japan) diameter and length, 3 mm and 100 mm, respectively; resistance, 0.5 MΩ; capacitance, 1.0 nF; loading current, 1-3 mA; applied voltage, 3 kV; and frequency, 300-800 Hz.

Simplified Hummer Solution: The solution contained 40 ml of H_2SO_4 and 1.8 g of $KMnO_4$. During the reaction, the color of the solution changed from dark purplish green to dark brown. To check the reaction process, H_2O_2 solution was added and the color of the solution changed to bright yellow, indicating the high oxidation level of graphite.

Instrumentation: The size distributions of the aerosol carriers were measured by a SMPS, consisting of a nano differential mobility analyzer (3085, TSI, US), condensation particle counter (3022A, TSI, US), and soft X-ray charger. The SMPS system, which measured the equivalent mobility diameter, was operated at a sample flow of 0.3 L min^{-1}, a sheath flow of 1.0 L min^{-1}, and a scan time of 135 sec (measurement range: 7.91-333.8 nm). TEM (JEM-3010, JEOL, Japan) images were obtained at an accelerating voltage range at 300 kV. Specimens were prepared for examination in the TEM by direct electrostatic aerosol sampling at a sampling flow of 1.0 L min^{-1} and an operating voltage of 5 kV using a Nano Particle Collector (NPC-10, HCT, Korea). An atomic force microscope (AFM, NanoScope IIIa, Veeco, US) was used for the topography of the GO. The drive frequency was 330 kHz, and the voltage was between 3.0 and 4.0 V. The drive amplitude was about 300 mV, and the scan rate was 0.5-1.0 Hz. X-ray diffraction studies of SnO_x-rGO were carried out on a Rigaku RINT-2100 diffractometer (Japan) equipped with a thin-film attachment using Cu-Kα radiation (40 kV, 40 mA). The 2θ angles ranged from 10° to 80° at 4°min^{-1} by step scanning

at an interval of 0.08°. FTIR spectra were recorded on a spectrometer (IFS 66/S, Bruker Optics, Germany) in the region of 4,000-600 cm^{-1} with a 0.1 cm^{-1} resolution.

Electrochemical performance: The electrochemical measurements were carried out using a LAND CT2001 A battery tester with lithium metal as the counter electrodes at room temperature. The fabricated SnO_x-rGO hybrid particles were mixed with PVDF, at the weight ratio of 90:10 in *N*-methyl-2-pyrrolidone to form a homogeneous black slurry. The resultant slurry was then pasted on copper foil substrate with a blade. The hybrid particles loading density of the electrode is *ca.* 1.0 mg cm^{-2}. The prepared electrode sheets were placed in a vacuum at 80 ^{o}C to evaporate the solvent. CR2032-type coin cells were fabricated in a glove box with an argon atmosphere. The lithium metal foil was used as the counter electrode. The electrolyte was 1 M $LiPF_6$ in a 50:50 *w*/*w* mixture of ethylene carbonate and diethyl carbonate. Charge-discharge cycles of the cells were measured at a constant current density of 50 mAg^{-1} within the voltage range of 0-2.0 V.

GO SYNTHESIS

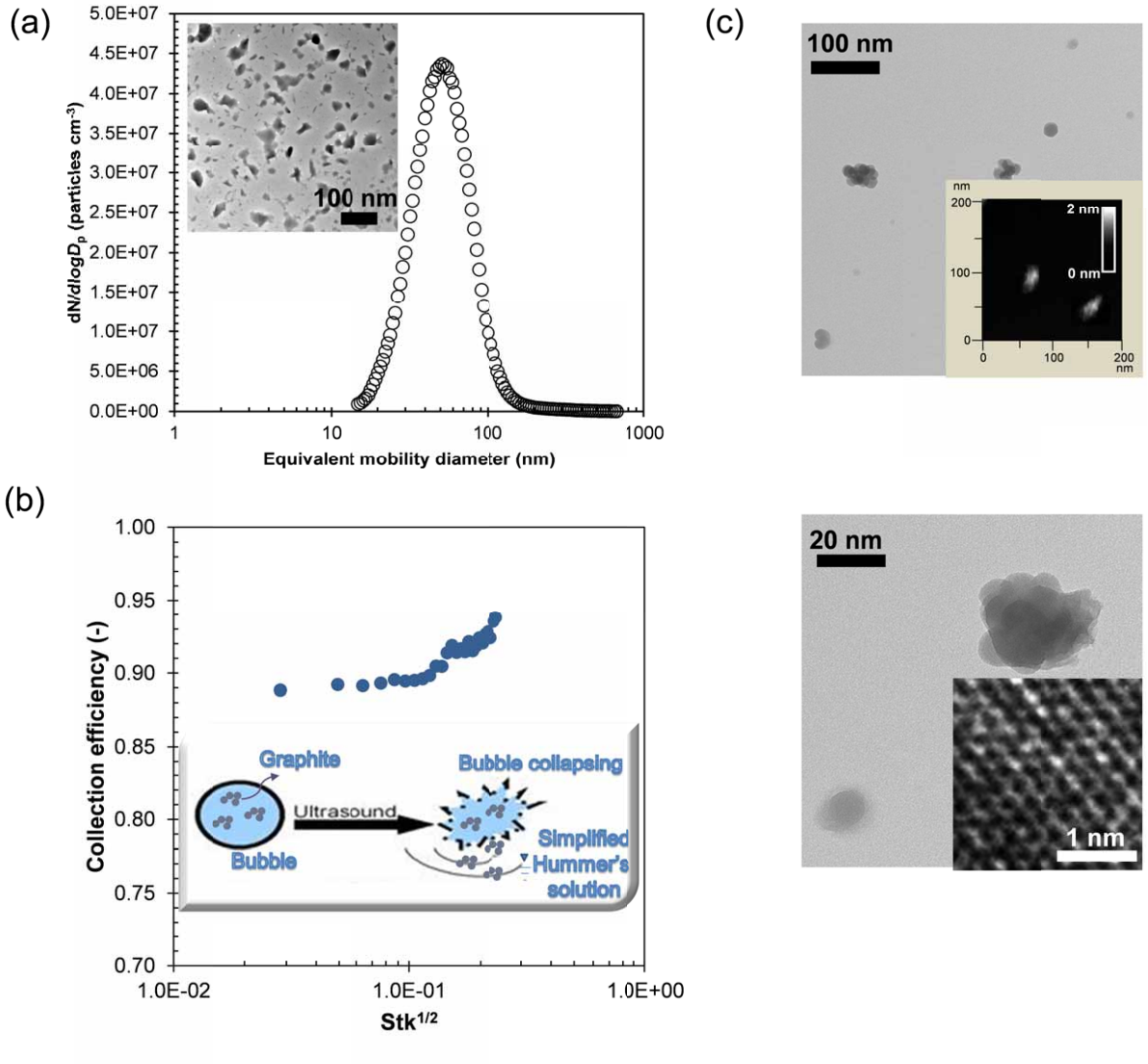

Figure S1. (a) The size distribution of the aerosol graphite particles, with an inset showing the TEM image. (b) The collection efficiency of aerosol graphite particles by an ultrasound impinging device. This figure also shows a schematic (inset) of the graphite collection by a bubble collapsing in the presence of ultrasound. (c) TEM and AFM images of GO particles after the simplified Hummer's reaction.

To prepare GO, first aerosol graphite nanoparticles were produced by spark discharge. The gas temperature inside the spark channel increased beyond a critical value, which was sufficient to sublimate parts of the graphite electrodes.[S1] The duration of each spark was very short (~1 msec) and the vapors cooled rapidly downstream of the spark. This formed a supersaturation resulting in particle formation through nucleation-condensation. The TNC, GMD, and GSD of the graphite particles, which were measured using a SMPS, were 2.00×10^7 particles cm^{-3}, 50.7 nm, and 1.54, respectively, as shown in Figure S1a. Figure S1a also shows a TEM image of the graphite particles. The mean mode diameter of the graphite particles was 56 ± 5.5 nm, and this was consistent with the aerosol size distribution described in Table SI. The generated aerosol graphite particles were carried using a flow of nitrogen gas

and then collected in the simplified Hummer solution by means of ultrasound. Figure S1b shows the collection efficiency of the graphite particles to be oxidized in the impinging device at 250 W cm^{-2} of ultrasound intensity. The particles experienced an ultrasound streaming at the gas-liquid interface and about 94% of the particles were collected in the ethanol solution, because the ultrasound streaming on the interface could give rise to a particle velocity (U_{as}) with the following equation:[S2]

$$U_{as} = \left(\frac{2P\beta}{\rho_g c_s \pi \alpha^2 X} \right)^{1/2} \quad \text{(S1)}$$

where P is the acoustic power of the ultrasound, β is the acoustic energy attenuation coefficient, ρ_g is the gas density, c_s is the sonic velocity in gas, α is the semi-angle of the spread of the streaming, and X is the distance from the source. The number of < 30nm particles was not significantly decreased, although the particles which are < 30 nm may be governed by diffusional behavior for the conventional impactors. This may have originated from different mechanisms of particle attachment on their counter media, between the present method [the particles in a bubble attached on the liquid surface by the bubble collapsing (refer to the inset of Figure S1b) due to ultrasound streaming] and the conventional method (the particles in gas attached on a solid plate by inertial impaction).[S3] The plots were generated by dividing the output and input aerosol size distribution. The reacted solution containing GO was atomized as droplets, and then passed through a denuder to separate the GO particles. The TNC, GMD, and GSD of the GO particles were 2.74×10^6 particles cm^{-3}, 36.2 nm, and 1.57, respectively; Figure S1c shows a TEM image of the GO particles (35 ± 4.9 nm). The morphology of the GO particles was in the form of flakes, and a high resolution TEM image (inset of Figure S1c) of the GO shows the regular hexagonal structure expected for graphene while several internal defects could also be found within the structure. Figure S1c also shows a representative AFM image of the GO particles on a silicon substrate. Their apparent thickness is about 1 nm, which indicates that they are single graphene layers.

Table SI A summary of the size distributions of aerosol graphite, GO, SnO_x, rGO, SnO_x-rGO (at 6 W), SnO_x-rGO (at 3 W), SnO_x-rGO (at 9 W), MoO_x-rGO (at 6 W), and NbO_x-rGO (at 6 W) particles

Case	GMD (nm)	GSD (-)	TNC ($\times 10^6$ particles cm^{-3})
Graphite	50.7	1.54	20.0
GO	36.2	1.57	2.74
SnO_x	33.8	1.47	5.81
rGO	34.5	1.52	2.35
SnO_x-rGO	31.8	1.47	3.03
3W	31.3	1.44	2.76
9W	35.2	1.51	4.87
MoO_x-rGO	35.7	1.58	3.36
NbO_x-rGO	35.0	1.53	3.31

XRD PATTERNS

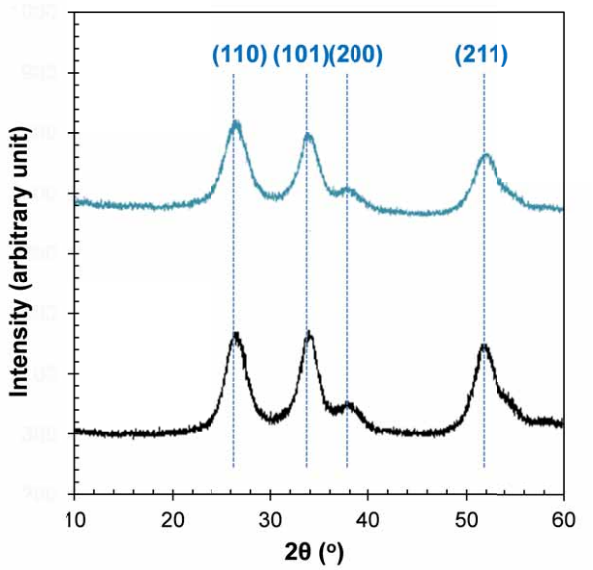

Figure S2. XRD patterns of SnO_x (black) and SnO_x-rGO (blue).

Figure S2 shows the XRD patterns of SnO_x and SnO_x-rGO. The diffraction peaks can be indexed to the standard tetragonal SnO_2 phase (JCPDS 72-1147), indicating that crystalline SnO_2 nanoparticles could be formed by the spark discharge. The broad diffraction peaks of the SnO_x-rGO suggest that the particles are ultrafine in size. No obvious diffraction peak attributed to graphite in the pattern of SnO_x-rGO was observed. This result indicates that the SnO_x particles decorated on rGO can prevent them from stacking into multilayers. The average crystal size of the SnO_x particles in SnO_x-rGO is around 3.8 nm, as calculated by Scherrer´s formula based on the (110) peak.

FTIR SPECTRA

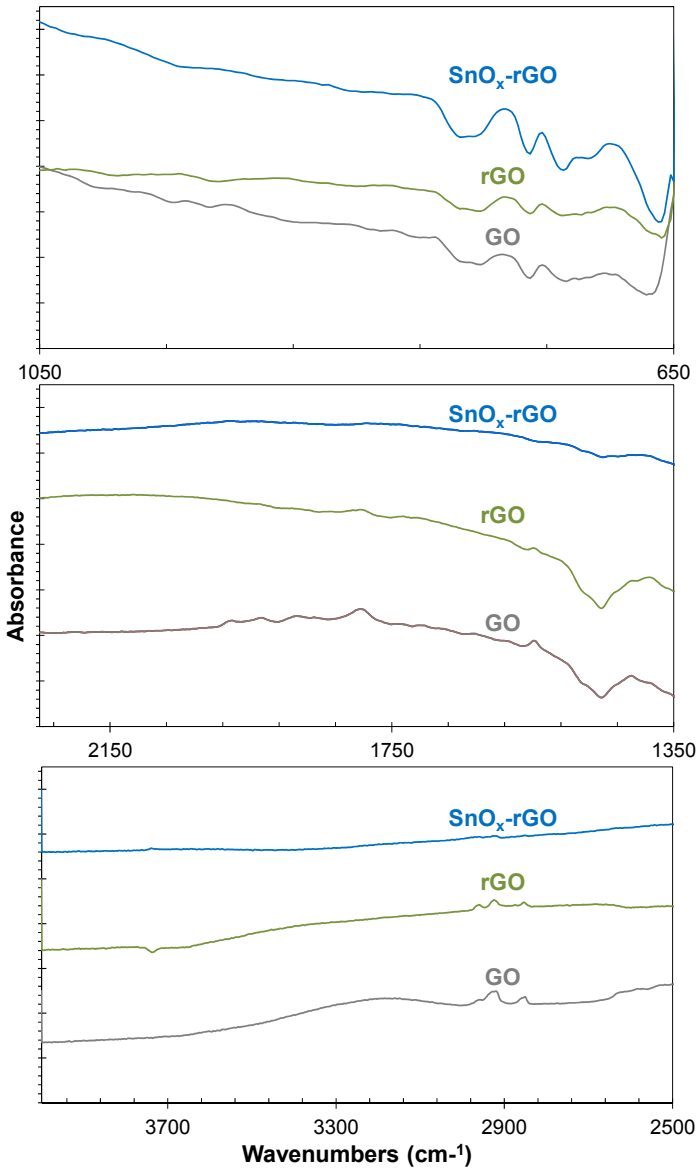

Figure S3. FTIR spectra of the GO, rGO, and SnO_x-rGO.

Analyses of GO, rGO, and SnO_x-rGO particles using Fourier transform infrared (FTIR) spectroscopy (Nicolet 6700, Thermo Electron, US) were performed to verify the structural differences between the samples. In Figure S3, the peak around 1,730 cm^{-1} was characteristic of C=O in carboxylic acid and carbonyl moieties on the surface of the GO, and the peaks at 1620, 1,410, 1,380, and 830 cm^{-1} were characteristic of aromatic C=C, carboxy C-O, O-H, and O-C=O groups, respectively. Other features include characteristic absorption peaks at around 3,300 cm^{-1} (related to O-H groups), 2,940 cm^{-1} (CH_2 bend), and 2,960 cm^{-1} (CH_3 bend). Compared with GO, rGO shows a featureless spectrum at the given absorbance scales, implying a reduction in the amount of oxygen functionalities. The spectrum of rGO was not significantly changed after the incorporation of SnO_x particles, but new bands around at 700 cm^{-1} which correspond to Sn-O and SnO_2 stretching, clarify that SnO_2 nanocrystals exist within the hybrid particles.[S4]

ADSORPTION ISOTHERMS

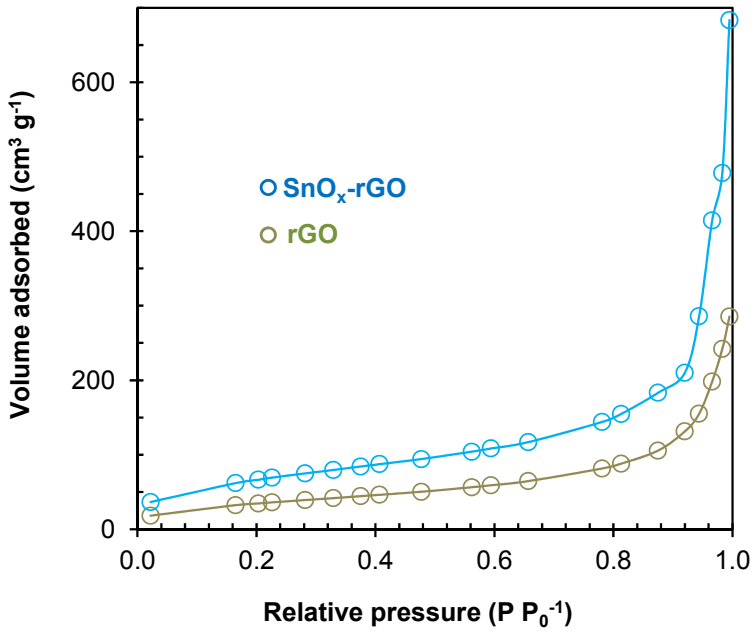

Figure S4. Adsorption isotherms of rGO and SnO_x-rGO.

Since the incorporated structure between SnO_x and rGO could result in a remarkable enhancement of the porosity, nitrogen adsoption isotherm measurements (Figure S4) have been carried out for SnO_x-rGO together with rGO. The isotherm for SnO_x-rGO was also found to be very similar to that of rGO, indicating that the porous structure of rGO was maintained even after the hybridization of the SnO_x particles. The Brunauer, Emmett, and Teller (BET) specific area of SnO_x-rGO is enhanced from 246 m^2 g^{-1} to 361 m^2 g^{-1} upon the hybridization between SnO_x and rGO. As a consequence, SnO_x-rGO could allow lithium ions and electrolyte molecules in entire sites on SnO_x and rGO particles as a result of the porous structure developed by hybridization. The pores within SnO_x-rGO could act as buffering spaces against the volume change of SnO_x particles upon the charge-discharge process, which eventually leads to enhanced cyclic performances in a LIB.

SUPPLEMENTARY REFERENCES

(S1) Byeon, J. H.; Kim, J.-W. *Appl. Phys. Lett.* **2010**, *96*, 153102.

(S2) Byeon, J. H.; Kim, Y.-W. *Nanoscale* **2012**, *4*, 6726.

(S3) Park, D.; Choi, N.-K.; Lee, S.-G.; Hwang, J. *Part. Part. Syst. Charact.* **2009**, *26*, 179.

(S4) Huang, X.; Zhou, X.; Zhou, L.; Qian, K.; Wang, Y.; Liu, Z.; Yu, C. *ChemPhysChem* **2011**, *12*, 278.